Dynamics of classical spins with dipolar coupling in a rigid lattice at high temperatures

S. J. Knak Jensen and E. Kjaersgaard Hansen
Department of Physical Chemistry, Chemical Institute, Aarhus University, DK-8000 Aarhus C, Denmark
(Received 16 June 1975)

Molecular-dynamics calculations have been performed on the auto- and pair time-correlation functions in a rigid lattice of magnetic dipoles coupled by a truncated dipolar interaction. The first six terms of the exact time expansion of the correlation functions calculated from first principles are also presented. The analytical forms of the autocorrelation functions are examined and compared to the predictions from a stochastic local-field model due to Kubo and Toyabe. The correlation functions are also used to probe the applicability of a theory of Blume and Hubbard to dipolar coupled spins. Generally, this theory describes the longitudinal dynamics rather well, whereas the transverse dynamics is less satisfactorily described.

I. INTRODUCTION

The free-induction decay (FID) has been used previously[1-3] to elucidate the dynamical properties of systems of magnetic dipoles. In this paper we report new information about the dynamical processes in a rigid lattice of dipolar coupled spins to supplement the FID. The results, which are obtained from molecular-dynamics experiments, are given in the form of auto- and pair time correlation functions between microscopic quantities, i.e., components of magnetic moments, whereas the FID represents the correlation function of the macroscopic magnetization.

The correlation functions derived from the molecular-dynamics experiments contain an error due to the limited number of systems in the Gibbsian ensemble. In order to estimate this experimental error, we have calculated the first six coefficients of the Taylor series expansion of the correlation functions (Sec. II). These coefficients are also useful in examining the character of the correlation functions for all values of the spin quantum number I (Sec. III), as well as in other connections.[4-6]

The correlation functions reported here may be used as a testing range for various models for the spin-relaxation processes, taken in the classical limit characteristic of the molecular-dynamics experiment. In Sec. IV we adapt Kubo and Toyabe's theory[7] for resonance line shapes to dipolar coupled spin systems and we compare the autocorrelation functions derived from this theory with those obtained from the molecular-dynamics experiments. Finally, in Sec. V we apply Blume and Hubbard's general theory[8] for spin correlation functions, originally developed for the Heisenberg model at high temperatures, to the spin system considered here and compare the obtained correlation functions with our results.

II. COMPUTATIONAL METHODS

We consider a system of N identical spins placed in a rigid simple-cubic lattice and subject to an external magnetic field $\vec{B}_0$ along the z axis. We assume that the high-temperature and high-field approximations[2] are valid for the spin system. The high-field approximation implies that only the terms of the truncated dipolar interaction H influence the line shapes considered here. H is given by

$$H=\frac{\gamma^2\hbar^2}{6}\sum_j^N\sum_k^N B_{jk}(3I_{jz}I_{kz}-\vec{I}_j\cdot\vec{I}_k), \tag{2.1}$$

where

$$B_{jk}=\tfrac{3}{2}(1-3\cos^2\theta_{jk})/r_{jk}^3,\quad j\neq k$$
$$B_{jj}=0. \tag{2.2}$$

γ is the magnetogyric ratio for the spins and θ_{jk} is the angle between $\vec{r}_{jk}$ and $\vec{B}_0$, where r_{jk} is the distance between spin j and k.

It proves convenient to write H as

$$H=-\tfrac{1}{2}\gamma\hbar\sum_j^N\vec{I}_j\cdot\vec{B}_j^{\rm loc} \tag{2.3}$$

where $\vec{B}_j^{\rm loc}$ has the components

$$B_{jp}^{\rm loc}=\begin{cases}\tfrac{1}{3}\gamma\hbar\sum_{k(\neq j)}^N B_{jk}I_{kp}, & p=x,y\\ -\tfrac{2}{3}\gamma\hbar\sum_{k(\neq j)}^N B_{jk}I_{kp}, & p=z.\end{cases} \tag{2.4}$$

It is well known that the FID may be written as[1]

$$F_x(t)=\langle M_x M_x(t)\rangle/\langle M_x^2\rangle, \tag{2.5}$$

where $\langle\cdots\rangle$ indicates an equilibrium ensemble average. M_x is the macroscopic magnetic moment

operator in the x direction:

$$M_x = \gamma\hbar \sum_j^N I_{jx} = \sum_j^N \mu_{jx}. \tag{2.6}$$

The FID may also be expressed as

$$F_x(t) = \frac{\langle \mu_{jx}\mu_{jx}(t)\rangle}{\langle \mu_{jx}^2\rangle} + \sum_{k=1(\neq j)}^{N} \frac{\langle \mu_{jx}\mu_{kx}(t)\rangle}{\langle \mu_{jx}^2\rangle}$$
$$\equiv f_x^{jj}(t) + \sum_{k=1(\neq j)}^{N} f_x^{jk}(t), \tag{2.7}$$

where j is an arbitrary spin. $f_x^{jj}(t)$ is the transverse autocorrelation function for a single spin and $f_x^{jk}(t)$ is the transverse pair correlation function involving the spins j and k.

The form of the Hamiltonian, Eq. (2.1), implies that $\langle M_z\rangle$, the macroscopic magnetic moment along $\vec{B}_0$, is a constant of motion so that

$$F_z(t) = \langle M_z M_z(t)\rangle / \langle M_z^2\rangle = 1. \tag{2.8}$$

In discussing the theories in Secs. IV and V it proves useful to write $F_z(t)$ in a way similar to Eq. (2.7)

$$F_z(t) = f_z^{jj}(t) + \sum_{k=1(\neq j)}^{N} f_z^{jk}(t). \tag{2.9}$$

In order to obtain the various correlation functions in Eqs. (2.7) and (2.9) by a molecular-dynamics experiment, we must confine the calculation to classical spins. In this limit, the time evolution of the spins is given by

$$\frac{d\vec{\mu}_j}{dt} = \gamma\, \vec{\mu}_j(t) \times \vec{B}_j^{\,\mathrm{loc}}(t), \tag{2.10}$$

where $\vec{\mu}_j$ is now considered a three-dimensional spatial vector, and $\vec{B}_j^{\,\mathrm{loc}}$ may be thought of as the local field at the position of the jth spin produced by the surrounding spins.

In the molecular-dynamics experiment the equations of motion, Eq. (2.10), are integrated numerically for an ensemble consisting of K systems, each containing $N = 12^3$ spins. The initial states of the systems must be selected so that they represent a Gibbsian ensemble at a prescribed temperature. Generally, the initial states may be found from a Monte Carlo procedure, which selects the systems so that the ensemble has certain thermodynamic properties, like the energy and the sublattice magnetization, corresponding to the given temperature. However, in the high-temperature limit, which we are discussing here, the initial states are completely disordered and the systems may be constructed simply by assigning random orientations to each of the spins in all systems. The integration of Eq. (2.10) was performed as described previously,[9] in particular the calculation of the local fields includes only the contribution from the 26 nearest neighbors. In the integration it is useful to express the time in the reduced unit

$$X = 2r_0^3/3\gamma|\vec{\mu}|, \tag{2.11}$$

where r_0 is the lattice spacing.

From the integration we obtain $\vec{\mu}_j^{\,\nu}(t_i)$, where the superscript indicates the particular system. The value of the correlation functions at time t_n may then be obtained by averaging $\mu_{jp}^{\nu}\mu_{kp}^{\nu}(t_n)$ over the ensemble, i.e., sum over ν However, we shall assume that the system is ergodic so that we may also average over different time origins, t_h, i.e., we shall sum $\mu_{jp}^{\nu}(t_h)\mu_{kp}^{\nu}(t_h + t_n)$ over t_h. In the actual time averaging we have not taken the contribution for each time increament Δt but rather for every $9\Delta t$ only, since this reduces the computing time substantially without altering the values of the normalized correlation function appreciably. This is due to the fact that the pair $\mu_{jp}^{\nu}(t_h)$ and $\mu_{kp}^{\nu}(t_h + t_n)$ contains essentially the same information as the pair $\mu_{jp}^{\nu}(t_{h+1})$ and $\mu_{kp}^{\nu}(t_{h+1} + t_n)$.

In the calculation of the pair correlation functions between the spins j and k we may also use the symmetry of the system to average $\mu_{jp}^{\nu}(t_h)\mu_{kp}^{\nu}(t_h + t_n)$ over all pairs of spins v and m which are equivalent to the pair j and k. For the autocorrelation functions we average over all N spins. Moreover, for transverse correlation functions we may also average over the x and y components. Accordingly, the normalized transverse correlation functions $f_x^{jj}(t)$ and $f_x^{jk}(t)$ may be calculated as

$$f_x^{jj}(t_n) = \frac{\sum_{\nu=1}^{K}\sum_{h=1}^{W}\sum_{k=1}^{N}\sum_{p=x,y}\mu_{kp}^{\nu}(t_h)\mu_{kp}^{\nu}(t_h + t_n)}{\sum_{\nu=1}^{K}\sum_{h=1}^{W}\sum_{k=1}^{N}\sum_{p=x,y}[\mu_{kp}^{\nu}(t_h)]^2}, \tag{2.12}$$

$$f_x^{jk}(t_n) = \frac{\sum_{\nu=1}^{K}\sum_{h=1}^{W}\sum_{(v,m)}\sum_{p=x,y}\mu_{vp}^{\nu}(t_h)\mu_{mp}^{\nu}(t_h + t_n)}{\sum_{\nu=1}^{K}\sum_{h=1}^{W}\sum_{(v,m)}\sum_{p=x,y}[\mu_{mp}^{\nu}(t_h)]^2}. \tag{2.13}$$

The longitudinal correlation functions, $f_z^{jj}(t)$ and $f_z^{jk}(t)$ are calculated in a similar way except that the sum over x,y is missing, i.e., $p = z$. The calculations were performed for $\vec{B}_0$ along the three "canonical" directions [001], [110], and [111].

In the actual calculation W was taken to be 50 in the transverse case whereas it was only 16 in the longitudinal case owing to the relatively slow decay of the longitudinal correlation functions. In order to reduce computing time K was chosen rather small, 8 for $\vec{B}_0$ along [001] and 4 in the rest of the cases except for the longitudinal case for $\vec{B}_0$ along [111], where K was 25.

In addition to the correlation functions derived from the molecular-dynamics experiments it is

also desirable to know the exact first few terms of the Taylor series expansion of the correlation functions. We calculate the equilibrium ensemble averages according to

$$\langle \cdots \rangle = \mathrm{Tr}(\rho_0 \cdots)/\mathrm{Tr}(\rho_0), \tag{2.14}$$

where ρ_0 is the high-temperature density matrix for the spin system. $f_p^{jj}(t)$ and $f_p^{jk}(t)(p=x,z)$ are then given by

$$f_p^{jj}(t) = \mathrm{Tr}(I_{jp} e^{iH^{\times}t/\hbar} I_{jp})/\mathrm{Tr}(I_{jp}^2) = 1 + \sum_{n=1}^{\infty} (-1)^n \frac{m_{2n,p}^{jj} t^{2n}}{(2n)!}, \tag{2.15}$$

$$f_p^{jk}(t) = \mathrm{Tr}(I_{jp} e^{iH^{\times}t/\hbar} I_{kp})/\mathrm{Tr}(I_{jp}^2) = \sum_{n=1}^{\infty} (-1)^n \frac{m_{2n,p}^{jk} t^{2n}}{(2n)!}, \tag{2.16}$$

where $H^{\times}$ is related to H in Eq. (2.1) by

$$H^{\times} \cdots = [H, \ldots]. \tag{2.17}$$

It may then be shown, by a procedure similar to the one given in Ref. 10, that the coefficients $m_{2n,p}^{jj}$ and $m_{2n,p}^{jk}$ are given by

$$m_{2n,p}^{jj} = (-\hbar^2)^{-n} \mathrm{Tr}\{[(H^{\times})^n I_{jp}][(H^{\times})^n I_{jp}]\}/\mathrm{Tr}(I_{jp}^2), \tag{2.18}$$

$$m_{2n,p}^{jk} = (-\hbar^2)^{-n} \mathrm{Tr}\{[(H^{\times})^n I_{jp}][(H^{\times})^n I_{kp}]\}/\mathrm{Tr}(I_{jp}^2). \tag{2.19}$$

All the quantum statistical operations and the necessary algebraic reductions involved in Eqs. (2.18) and (2.19) are performed on a computer as described elsewhere[10] and the analytical expressions for the coefficients are given in the Appendix. We note that the coefficients calculated in this way are valid for all values of the spin quantum number I, not only for classical spins.

The computations were performed on the CDC 6400 Computer at RECAU, The Regional Computing Center at Aarhus University.

III. EXPERIMENTAL CORRELATION FUNCTIONS

A representative set of correlation functions is shown in Figs. 1–4. Before we use these functions to examine the theories described in Secs. IV and V we want to discuss some of the properties of the correlation functions.

A. Transverse correlation functions

The reliability of the autocorrelation functions $f_x^{jj}(t)$ is investigated by calculating experimental values of $m_{2,x}^{jj}, m_{4,x}^{jj}, m_{6,x}^{jj}$ from the Fourier transform of $f_x^{jj}(t)$ and comparing them to the exact values in Table I. The difference between the two sets of values is on the average 0.4%, 1%, and 3% for $m_{2,x}^{jj}$, $m_{4,x}^{jj}$, and $m_{6,x}^{jj}$, respectively.

The autocorrelation functions in Fig. 1 are positive for all three directions of $\vec{B}_0$ without the large oscillations characteristic of the FID. This implies that the oscillations of the FID may be ascribed to pair correlation functions of the spins. In fact, the functional form of $f_x^{jj}(t)$ is well represented by the Gaussian function $\exp(-m_{2,x}^{jj} t^2/2)$ for times $t \leq 2.7(m_{2,x}^{jj})^{-1/2}$. The Gaussian character is also apparent in the ratio of coefficients

$$D_{2n,x} = m_{2n,x}^{jj}/(m_{2,x}^{jj})^n. \tag{3.1}$$

If $f_p^{jj}(t)$ were a Gaussian function then $D_{2n,p}$ would be given by

$$D_{2n,p} = (2n)!/(2^n n!) \quad (p = x,y,z). \tag{3.2}$$

Numerical values of $D_{2n,p}$ are found in Table II, from which it is seen that for classical spins $D_{4,x}$ and $D_{6,x}$ deviate from the Gaussian values (3 and 15) by 1% and 7% on the average, respectively. Table II also list $D_{4,x}$ and $D_{6,x}$ for a spin-$\frac{1}{2}$ system. In this case $D_{4,x}$ and $D_{6,x}$ deviate from the Gaussian values by 3% and 8% on the average, implying that the Gaussian form of $f_x^{jj}(t)$ may very well also hold for quantum-mechanical spin systems. The transverse pair correlation functions in Fig. 2 have a small finite value at $t=0$ due to the restricted number of systems applied in the ensemble averaging process. The experimental values of the coefficients $m_{2,x}^{jk}$, $m_{4,x}^{jk}$, and $m_{6,x}^{jk}$ deviate from the exact values in Table III by 7%, 13%, and 28% on the average. Generally, the pair correla-

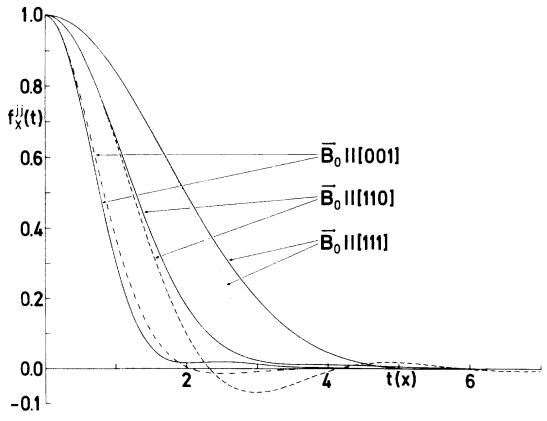

FIG. 1. Transverse autocorrelation functions for classical spins with truncated dipolar interaction in a simple cubic lattice. Solid line: molecular-dynamics experiments; dotted line: Taylor series expansion incorporating the terms up to t^6; dashed line: the Blume-Hubbard model; dot-dashed line: the Kubo-Toyabe model. The time is in units of $X = 2r_0^3/3\gamma|\tilde{\mu}|$.

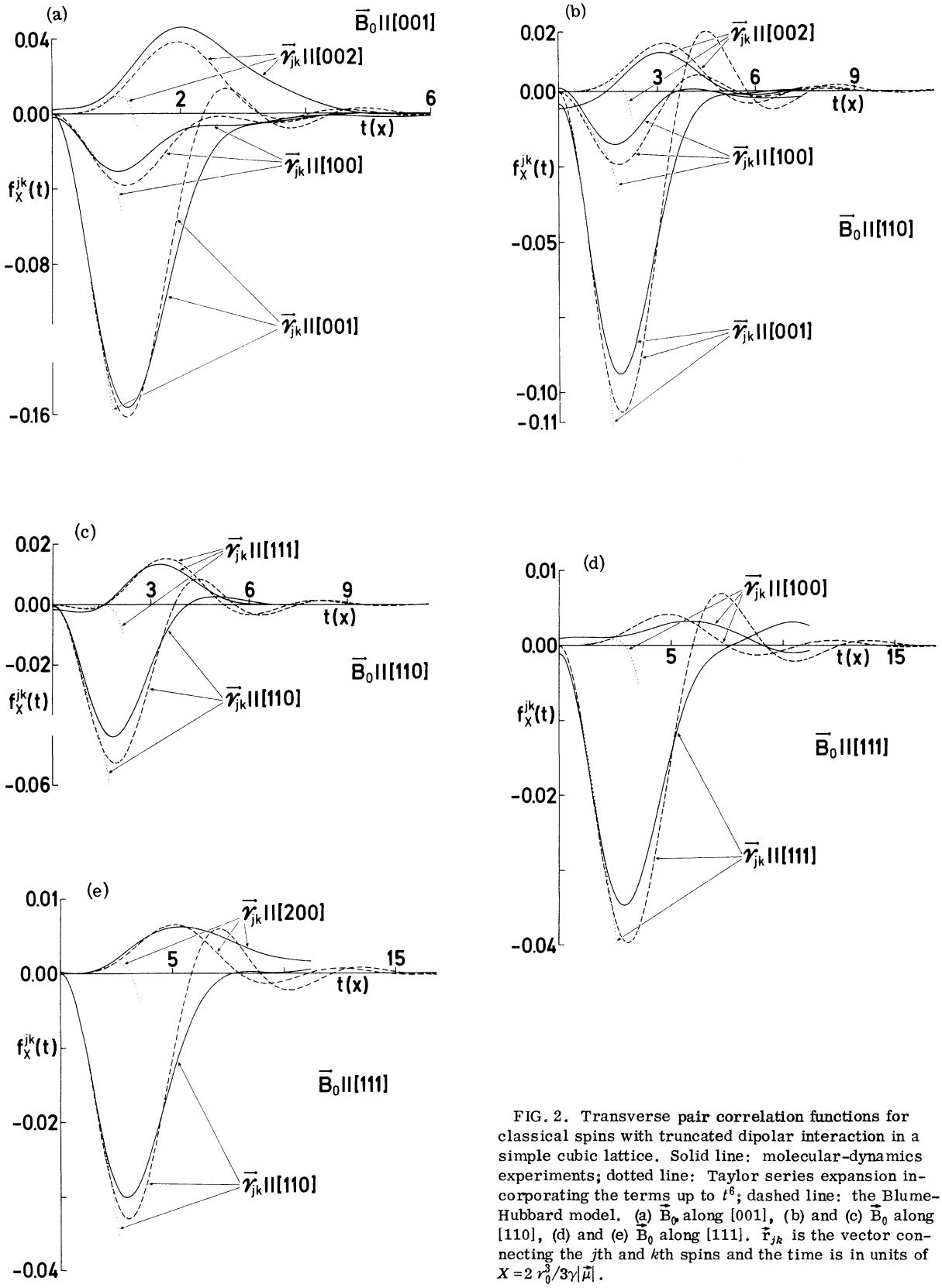

FIG. 2. Transverse pair correlation functions for classical spins with truncated dipolar interaction in a simple cubic lattice. Solid line: molecular-dynamics experiments; dotted line: Taylor series expansion incorporating the terms up to t^6; dashed line: the Blume-Hubbard model. (a) $\vec{B}_0$ along [001], (b) and (c) $\vec{B}_0$ along [110], (d) and (e) $\vec{B}_0$ along [111]. $\vec{r}_{jk}$ is the vector connecting the jth and kth spins and the time is in units of $X = 2\,r_0^3/3\gamma|\vec{\mu}|$.

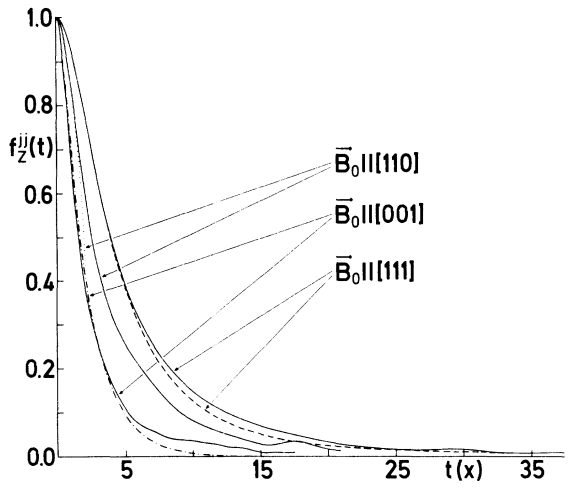

FIG. 3. Longitudinal autocorrelation functions for classical spins with truncated dipolar interaction in a simple cubic lattice. The symbols are explained in Fig. 1.

tion functions have one relatively large extremum value and in some cases a few smaller ones.

Figures 2(a)–2(e) show which of the pair correlation functions gives the largest contribution to the first negative region of the FID. For $\vec{B}_0$ along [001] and [110] this comes from the pair correlation between the nearest neighbors along [001], i.e., those spins with the strongest interaction. This is not so for $\vec{B}_0$ along [111] since in this case there is no direct interaction between these spins ($B_{jk}=0$) and therefore $f_x^{jk}(t)$ takes on small values only. For this orientation of $\vec{B}_0$, the largest contribution stems from the correlation functions involving the spins along [111] and [110].

In Fig. 5 we show how the FID is constructed as the sum of the 26 nearest-neighbor pair correlation functions and the autocorrelation function and it is compared to a FID which incorporates all pair correlations in a lattice with 216 spins. Although the FID obtained in this way displays the usual oscillatory behavior, the amplitude at the first minimum is off by 45%, indicating the importance of correlation functions between more distant spins than the 26 nearest, even at the position of the first minimum.

B. Longitudinal correlation functions

The longitudinal autocorrelation functions in Fig. 3 are positive like the transverse correlation functions, but otherwise the forms of $f_x^{jj}(t)$ and $f_z^{jj}(t)$ are rather different. The short-time Gaussian form only extends up to $t \leq 0.5\ (m_{2,z}^{jj})^{-1/2}$, which also is clearly indicated in the $D_{2n,z}$ values in Table II, both for classical- and quantum-mechanical spin systems. For intermediate times the functional form of $f_z^{jj}(t)$ is somewhat similar of an exponential decay. The long-time behavior of $f_z^{jj}(t)$ is best examined for $\vec{B}_0$ along [111] since this function incorporates more systems in the averaging process than the other two. In this direction $f_z^{jj}(t)$ may for long times be represented by

$$f_z^{jj}(t) = \prod_{i=1}^{3} (2\pi)^{-1} \int_{-\infty}^{\infty} e^{-q_i^2 D_i t}\, dq_i$$

$$= (64\pi^3 D_1 D_2 D_3)^{-1/2} t^{-3/2}, \tag{3.3}$$

where D_1, D_2, and D_3 are the principal values of the spin-diffusion tensor. The theoretical values of D_i, which give the best agreement[11] with our data are those based on the Blume-Hubbard model in Sec. V. The numerical values of D_i are listed in Table IV. The experimental values of the coefficients $m_{2,z}^{jj}$, $m_{4,z}^{jj}$, and $m_{6,z}^{jj}$ deviate from the exact values in Table I by 1%, 6%, and 16% on the average.

The longitudinal pair correlations functions have in some cases a small negative value at $t=0$ related to the smallness of the ensemble, but apart from this, $f_z^{jk}(t)$ are positive in the time region investigated—in contrast to the transverse pair correlation functions. The $f_z^{jk}(t)$ oscillates at times large enough for the corresponding transverse pair correlation functions to have decayed to zero. These oscillations, which are due to the small number of systems applied in the averaging process, prevent the determination of experimental values of $m_{2n,z}^{jk}$. The longitudinal pair correlation functions, which have the largest maximum value for $\vec{B}_0$ along [001] and [110], involve the same spins as have the largest minimum value for the transverse paircorrelation functions, i.e., those spins for which $\vec{r}_{jk}$ is along [001].

IV. STOCHASTIC DESCRIPTION OF THE SPIN MOTION

The classical equation of motion for the spins, Eq. (2.10), shows that the local field acting on a given dipole, $\vec{\mu}_j(t)$, is a function of the orientation of the dipole itself at times prior to t, because the orientation of dipoles neighboring to $\vec{\mu}_j$ is determined in part by the previous orientations of $\vec{\mu}_j$. However, we may argue that since many spins interact simultaneously with a given neighboring dipole we may neglect this detailed dependence and assume that the local field is not dependent upon $\vec{\mu}_j$ and, consequently, treat the local field as a stochastic process, $\vec{B}(t)$. Using this approximation we may write the equation of motion for a single spin $\vec{I}$ as

$$\frac{d\vec{I}}{dt} = \gamma \vec{I} \times \vec{B}(t). \tag{4.1}$$

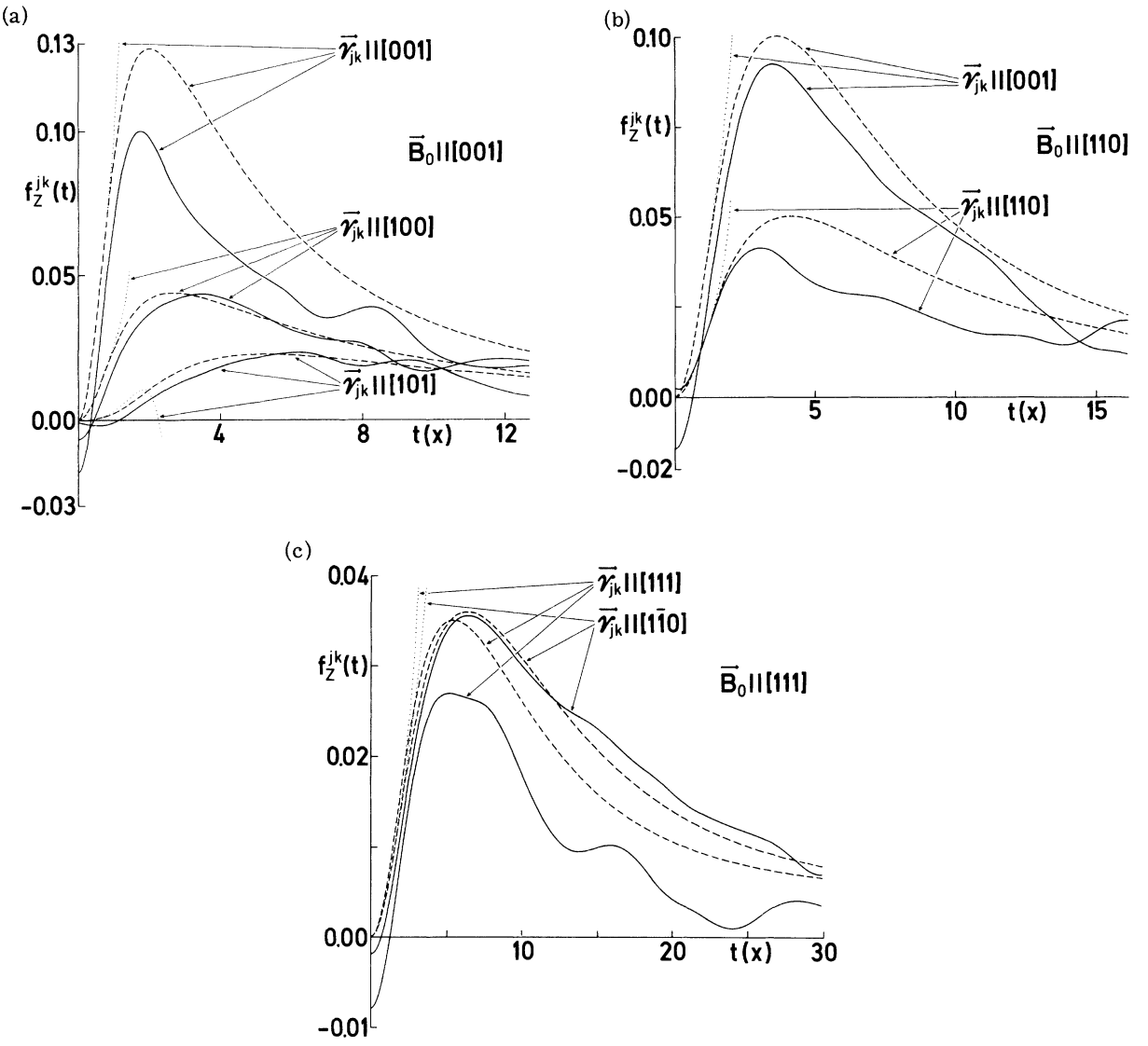

FIG. 4. Longitudinal pair correlation functions for classical spins with truncated dipolar interaction in a simple-cubic lattice. (a) $\vec{B}_0$ along [001], (b) $\vec{B}_0$ along [110], (c) $\vec{B}_0$ along [111]. The symbols are explained in Fig. 2.

Kubo and Toyabe[7] (KT) have considered the problem of obtaining the spin autocorrelation functions from assumed properties of the stochastic nature of $\vec{B}(t)$ in addition to Eq. (4.1). In this selection we shall adapt their method to the system of dipolar coupled spins in order to compare the predictions of the stochastic theory with the results of the molecular-dynamics experiments.

KT make the simplifying assumption that the components of $\vec{B}$ are independent stationary Gaussian and Markoffian processes, so that by the aid of Doob's theorem[12] it follows

$$\langle B_p B_{p'}(t)\rangle = (\Delta_p^2/\gamma^2)e^{-t/\tau_p}\delta_{p,p'}, \tag{4.2}$$

where τ_p is the correlation time for the local field and Δ_p is a measure of the local field amplitude. KT assume that τ_p and Δ_p are independent of p. For dipolar coupled spins, however, this assumption is not valid. In fact we see from Eq. (2.4) that

$$\langle B_p^{\rm loc} B_p^{\rm loc}\rangle \equiv \frac{\Delta_p^2}{\gamma^2} = \begin{cases} \frac{1}{27}\gamma^2\hbar^2 I(I+1)S_2, & p=x,y \\ \frac{4}{27}\gamma^2\hbar^2 I(I+1)S_2, & p=z \end{cases} \tag{4.3}$$

where $S_2 = \sum_{k(\neq j)} B_{jk}^2$.

Furthermore, using Eq. (2.4) we may express the exact time dependence of the normalized local-field correlation function as

TABLE I. Numerical values of the coefficients $m_{2n,p}^{jj}$, $p=x,z$, evaluated for a simple-cubic lattice in the limit $I\to\infty$, $\hbar\to 0$, while $I\hbar$ remains finite. Each spin interacts with 26 neighbors. $m_{2n,p}^{jj}$ is given in units of $(2r_0^3/3\gamma|\vec{\mu}|)^{-2n}$. A: exact coefficients, B: coefficients derived from the Blume-Hubbard model with $N=216$ [Eqs. (5.25) and (5.26)].

Direction of $\vec{B}_0$	$m_{2,x}^{jj}$		$m_{4,x}^{jj}$		$m_{6,x}^{jj}$		$m_{2,z}^{jj}$		$m_{4,z}^{jj}$		$m_{6,z}^{jj}$	
	A	B	A	B	A	B	A	B	A	B	A	B
[001]	2.3611	2.3611	16.443	14.171	198.38	137.41	0.944 44	0.944 44	5.4614	5.5498	70.328	68.640
[110]	0.853 48	0.853 48	2.2037	1.8013	10.006	6.2190	0.341 39	0.341 39	0.698 68	0.731 04	3.2757	3.3551
[111]	0.350 94	0.350 94	0.374 62	0.300 69	0.732 26	0.426 57	0.140 37	0.140 37	0.125 91	0.119 51	0.269 25	0.220 96

$$\langle B_p^{\rm loc}B_p^{\rm loc}(t)\rangle/\langle B_p^{\rm loc}B_p^{\rm loc}\rangle = f_p^{jj}(t)+\sum_{k,m\,(k\neq m)}(B_{jk}B_{jm}/S_2)f_p^{km}(t). \tag{4.4}$$

Equation (4.4) predicts that

$$\frac{d}{dt}\frac{\langle B_p^{\rm loc}B_p^{\rm loc}(t)\rangle}{\langle B_p^{\rm loc}B_p^{\rm loc}\rangle}\bigg|_{t=0}=0, \tag{4.5}$$

whereas the stochastic model gives

$$\frac{d}{dt}\frac{\langle B_p B_p(t)\rangle}{\langle B_p B_p\rangle}\bigg|_{t=0}=-\tau_p^{-1}\neq 0, \tag{4.6}$$

that is, the short-time dependence of the correlation function for the local field is incorrect. However, this short-time dependence is not very important for the short-time dependence of the spin correlation functions.

Let $P(\vec{I},\vec{B},t)$ be the probability density of the random variables $\vec{I}$ and $\vec{B}$ at time t. Following KT we may write the equation describing the time evolution of $P(\vec{I},\vec{B},t)$ as

$$\frac{\partial P(\vec{I},\vec{B},t)}{\partial t}=-\frac{d\vec{I}}{dt}\cdot\nabla_{\vec{I}}P(\vec{I},\vec{B},t)+\Gamma P(\vec{I},\vec{B},t), \tag{4.7}$$

where the operator Γ is

$$\Gamma=\sum_{p=x,y,z}\tau_p^{-1}\left(\frac{\Delta_p^2}{\gamma^2}\frac{\partial^2}{\partial B_p^2}+\frac{\partial}{\partial B_p}B_p\right). \tag{4.8}$$

The autocorrelation function $f_p(t)$ [$=f_p^{jj}(t)$] for the spin $\vec{I}$ may be expressed in terms of $P(\vec{I},\vec{B},t)$ by

$$f_p(t)=\frac{\langle I_p(0)I_p(t)\rangle}{\langle I_p^2\rangle} =\mathrm{Tr}\left(\int d^3B\int d^3I\,I_p(0)I_p P(\vec{I},\vec{B},t)\right)\Big/\mathrm{Tr}(I_p^2). \tag{4.9}$$

It is convenient to find $f_p(t)$ by first calculating its Fourier transform

$$g_p(\omega)=(2\pi)^{-1}\int_{-\infty}^{\infty}f_p(t)e^{i\omega t}dt =\pi^{-1}\,\mathrm{Re}\left[\mathrm{Tr}\left(\int d^3B\,I_p(0)J_p(\vec{B},\omega)\right)\right]\Big/\mathrm{Tr}(I_p^2), \tag{4.10}$$

where $J_p(\vec{B},\omega)$ is the pth component of

$$\vec{J}(\vec{B},\omega)=\int_0^{\infty}dt\,e^{i\omega t}\int d^3I\,\vec{I}P(\vec{I},\vec{B},t). \tag{4.11}$$

Multiplying Eq. (4.7) by $\int_0^{\infty}dt\,e^{i\omega t}\int d^3I\,\vec{I}$ and performing the integrations, we obtain the following equation for $\vec{J}(\vec{B},\omega)$

TABLE II. Ratio of the exact coefficients $D_{2n,p} = m^{jj}_{2n,p}/(m^{jj}_{2,p})^n$ in a simple-cubic lattice. A: A system of classical spins ($I \to \infty$, $\hbar \to 0$, $I\hbar$ finite), each spin interacts with 26 nearest neighbors. B: A system with spin $\frac{1}{2}$, each spin interacts with 342 neighbors.

Direction of $\vec{B}_0$	$D_{4,x}$		$D_{6,x}$		$D_{4,z}$		$D_{6,z}$	
	A	B	A	B	A	B	A	B
[001]	2.95	2.81	15.1	12.9	6.12	5.24	83.5	58.9
[110]	3.03	2.97	16.1	15.0	5.99	5.34	82.3	65.2
[111]	3.04	3.05	16.9	16.6	6.39	5.78	97.3	79.8

$$(-i\omega - \Gamma)\vec{J}(\vec{B},\omega) + \gamma \vec{B}\times\vec{J}(\vec{B},\omega) = \int d^3I\,\vec{I}P(\vec{I},\vec{B},0) = \vec{I}(0)P_0(\vec{B}), \tag{4.12}$$

where we have used in the last step the initial condition

$$P(\vec{I},\vec{B},0) = \delta(\vec{I}-\vec{I}(0))P_0(\vec{B}) \tag{4.13}$$

and $P_0(\vec{B})$ is the static distribution for $\vec{B}$

$$P_0(\vec{B}) = \prod_{p=x,y,z} \gamma \exp(-\tfrac{1}{2}\gamma^2 B_p^2/\Delta_p^2)/[(2\pi)^{1/2}\Delta_p]. \tag{4.14}$$

It is computionally advantageous to multiply Eq. (4.12) by

$$\Omega = \prod_{p=x,y,z} \exp[(\tfrac{1}{2}\gamma B_p/\Delta_p)^2] \tag{4.15}$$

which leads to

$$(-i\omega - \Gamma')\vec{J}'(\vec{B},\omega) + \gamma\vec{B}\times\vec{J}'(\vec{B},\omega) = \vec{I}(0)P_0'(\vec{B}), \tag{4.16}$$

where

$$\vec{J}'(\vec{B},\omega) = \Omega\vec{J}(\vec{B},\omega)$$

$$\Gamma' = \Omega\Gamma\Omega^{-1} = \sum_{p=x,y,z} \tau_p^{-1}\left[\frac{\Delta_p^2}{\gamma^2}\frac{\partial^2}{\partial B_p^2} - \frac{1}{4}\left(\frac{\gamma^2}{\Delta_p^2}\right)B_p^2 + \frac{1}{2}\right]$$

$$P_0'(\vec{B}) = \prod_{p=x,y,z} \gamma \exp[-(\tfrac{1}{2}\gamma B_p/\Delta_p)^2]/[(2\pi)^{1/2}\Delta_p]. \tag{4.17}$$

$g_p(\omega)$ may now be written as

$$g_p(\omega) = (\pi)^{-1}\mathrm{Re}\left[\mathrm{Tr}\left(\int d^3B I_p(0)\Omega^{-1}J_p'(\vec{B},\omega)\right)\right]\Big/\mathrm{Tr}(I_p^2). \tag{4.18}$$

Since Γ' is closely related to the Hamiltonian for a three-dimensional harmonic oscillator we shall expand $J_p'(\vec{B},\omega)$ in harmonic-oscillator eigenfunc-

TABLE III. Numerical values of the coefficients $m^{jk}_{2n,p}$, $j \neq k$, $p = x, z$ evaluated for a simple-cubic lattice. $\vec{r}_{jk}$ is the vector between the spins j and k and Q_k is the number of spins, which are in equivalent positions with respect to the jth spin. Each spin interacts with 26 neighbors and the moments are evaluated in the limit $I \to \infty$, $\hbar \to 0$, while $I\hbar$ remains finite. $m^{jk}_{2n,p}$ is given in units of $(2r_0^3/3\gamma|\vec{\mu}|)^{-2n}$.

Direction of $\vec{B}_0$	Direction of $\vec{r}_{jk}$	Q_k	$m^{jk}_{1,x}$	$m^{jk}_{1,z}$	$m^{jk}_{2,x}$	$m^{jk}_{2,z}$	$m^{jk}_{3,z}$	$m^{jk}_{4,z}$
[001]	[001]	2	0.592 59	5.109 95	59.130 87	−0.296 30	−2.229 56	−30.164 66
[001]	[100]	4	0.148 15	1.664 78	25.124 10	−0.074 07	−0.396 95	−3.519 01
[001]	[110]	4	0.018 52	0.279 12	4.745 73	−0.009 26	−0.056 88	−0.808 78
[001]	[101]	8	0.004 63	0.301 18	5.255 87	−0.002 31	0.050 34	0.326 11
[001]	[111]	8	0.	0.037 04	0.922 32	0.	0.009 26	0.101 96
[110]	[001]	2	0.148 148	0.534 679	2.617 519	−0.074 074	−0.161 391	−0.620 027
[110]	[100]	4	0.037 037	0.157 748	0.864 564	−0.018 519	−0.041 015	−0.172 052
[110]	[110]	2	0.074 074	0.273 214	1.334 830	−0.037 037	−0.108 410	−0.610 360
[110]	[1$\bar{1}$0]	2	0.018 519	0.087 088	0.509 911	−0.009 259	−0.017 268	−0.062 828
[110]	[101]	8	0.001 157	0.021 685	0.155 031	−0.000 579	0.003 012	0.010 363
[110]	[111]	4	0.005 487	0.051 007	0.307 101	−0.002 743	−0.002 482	−0.040 276
[110]	[1$\bar{1}$1]	4	0.005 487	0.031 138	0.191 170	−0.002 743	−0.006 660	−0.039 786
[111]	[001]	6	0.	0.001 625 8	0.005 668 9	0.	0.000 406 4	0.001 114 7
[111]	[110]	6	0.018 518 5	0.026 640 2	0.053 858 5	−0.009 259 3	−0.012 352 9	−0.032 676 4
[111]	[1$\bar{1}$0]	6	0.018 518 5	0.033 155 9	0.079 908 8	−0.009 259 3	−0.006 865 9	−0.008 278 1
[111]	[111]	2	0.021 947 9	0.032 830 5	0.068 098 1	−0.010 973 9	−0.011 938 4	−0.024 458 7
[111]	[1$\bar{1}$1]	6	0.002 438 7	0.003 752 5	0.008 363 0	−0.001 219 3	−0.001 364 5	−0.002 942 8

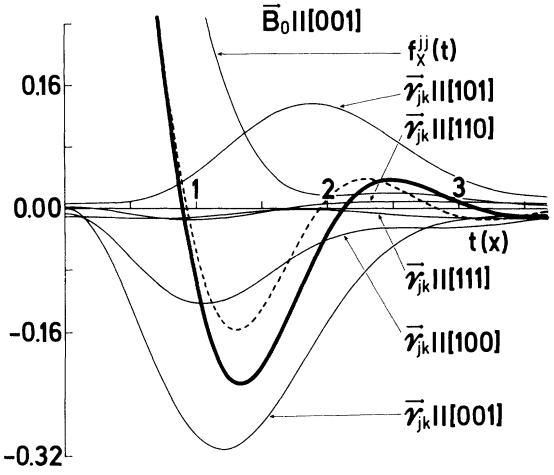

FIG. 5. Construction of the free-induction-decay line shape (heavy line) from the transverse autocorrelation function, $f_x^{jj}(t)$ (solid line), and the pair correlation functions, $f_x^{jk}(t)$ (solid line), of the 26 nearest neighbors. The symmetry of the spin system is used to group the 26 pair correlation functions into five sets, each set containing correlation functions between the jth spin and those spin k, which are in equivalent positions with respect to the jth spin. The pair correlation functions shown are the sum of the correlation functions in each of the five sets and they are labeled by a vector $\vec{r}_{jk}$ connecting one of the equivalent spin pairs in the set. Dashed line: free-induction-decay line shape from Ref. 9. The time is in units of $X = 2r_0^3/3\gamma|\vec{\mu}|$.

tions:

$$J_p'(\vec{B},\omega) = \sum_{n_x,\,n_y,\,n_z=0}^{\infty} \sum_{p'=x,y,z} C(p,p',n_x,n_y,n_z,\omega) \times F_{n_x,\,n_y,\,n_z}(\vec{B}) I_{p'}(0), \tag{4.19}$$

where $F_{n_x,n_y,n_z}(\vec{B})$ is a set of orthonormal eigenfunctions for Γ':

$$\Gamma' F_{n_x,n_y,n_z}(\vec{B}) = -E_{n_x,n_y,n_z} F_{n_x,n_y,n_z}(\vec{B}), \tag{4.20}$$

$$E_{n_x,n_y,n_z} = \sum_{p=x,y,z} \frac{n_p}{\tau_p}. \tag{4.21}$$

Substituting Eq. (4.19) into Eq. (4.18) leads to

$$g_p(\omega) = 2^{3/4}\pi^{-1/4}(\Delta_x\Delta_y\Delta_z)^{1/2}\gamma^{-3/2} \times \mathrm{Re}[C(p,p,0,0,0,\omega)], \tag{4.22}$$

since $F_{0,0,0}(\vec{B})$ is given by

$$F_{0,0,0}(\vec{B}) = (2\pi)^{-3/4}\gamma^{3/2}(\Delta_x\Delta_y\Delta_z)^{-1/2}\Omega^{-1}. \tag{4.23}$$

We shall now derive a set of equations for the C's in Eq. (4.19), which allows a determination of $C(p,p,0,0,0,\omega)$. We substitute Eq. (4.19) into the pth component of Eq. (4.16), multiply the resulting expression by $I_p(0)F_{n_x,n_y,n_z}(\vec{B})$, and perform the trace and integration $\int d^3B$. For the xth component of Eq. (4.16) this leads to

$$(-i\omega + E_{n_x,n_y,n_z})C(x,p,n_x,n_y,n_z,\omega) + \Delta_y[n_y^{1/2}C(z,p,n_x,n_y-1,n_z,\omega) + (n_y+1)^{1/2}C(z,p,n_x,n_y+1,n_z,\omega)] - \Delta_z[n_z^{1/2}C(y,p,n_x,n_y,n_z-1,\omega) + (n_z+1)^{1/2}C(y,p,n_x,n_y,n_z+1,\omega)] = (2\pi)^{-3/4}\gamma^{3/2}(\Delta_x\Delta_y\Delta_z)^{-1/2}\delta_{p,x}\delta_{n_x,0}\delta_{n_y,0}\delta_{n_z,0}. \tag{4.24}$$

In the calculation of Eq. (4.24) we have used properties of harmonic oscillator eigenfunctions like

$$\gamma B_y F_{n_x,n_y,n_z}(\vec{B}) = \Delta_y[(n_y+1)^{1/2}F_{n_x,n_y+1,n_z}(\vec{B}) + n_y^{1/2}F_{n_x,n_y-1,n_z}(\vec{B})]. \tag{4.25}$$

Equation (4.24) and the corresponding equations for the y and z components of Eq. (4.16) have the form of an infinite set of linear equations in the C's. This set of equations may be solved analytically in the limit of infinite frequencies giving

$$\lim_{\omega\to\infty} g_x(\omega) = (1/\pi)(\Delta_z^2\tau_z^{-1} + \Delta_y^2\tau_y^{-1})\omega^{-4}, \tag{4.26}$$

$$\lim_{\omega\to\infty} g_z(\omega) = (2/\pi)\Delta_x^2\tau_x^{-1}\omega^{-4}, \tag{4.27}$$

which for an isotropic interaction reduces to Anderson's result.[13] For finite frequencies we resort to a numerical procedure retaining only those equations of the set Eq. (4.24), which have $n_x + n_y$

TABLE IV. Components $D_{p,p'}$ $(p,p'=x,y,z)$ and eigenvalues D_1, D_2, and D_3 of the spin diffusion tensor calculated from the Blume-Hubbard model [Eq. (5.28) with N=216] for a simple-cubic lattice of classical spins ($I\to\infty$, $\hbar\to 0$, and $I\hbar$ finite). Each spin interacts with 26 nearest neighbors. $D_{p,p'}$ is given in units of $3\gamma|\vec{\mu}|/(2r_0)$.

Direction of $\vec{B}_0$	$D_{x,x}$	$D_{y,y}$	$D_{z,z}$	$D_{x,y}$	$D_{x,z}$	$D_{y,z}$	D_1	D_2	D_3
[001]	0.055 26	0.055 26	0.188 74	0.	0.	0.	0.055 26	0.055 26	0.188 74
[110]	0.067 89	0.067 89	0.083 55	0.024 55	0.	0.	0.092 45	0.043 34	0.083 55
[111]	0.075 79	0.075 79	0.075 79	0.014 55	0.014 55	0.014 55	0.061 24	0.061 24	0.104 89

$+n_z \leq 11$. The only parameters entering into the calculation are Δ_p and τ_p ($p = x, y, z$) through E_{n_x, n_y, n_z}. Δ_p is taken from Eq. (4.3) and τ_p may be estimated by expanding Eq. (4.4) as

$$\frac{\langle B_p^{\rm loc} B_p^{\rm loc}(t)\rangle}{\langle B_p^{\rm loc} B_p^{\rm loc}\rangle} = 1 - 1/2\left(m_{2,p}^{jj} + \sum_{k, m(k \neq m)} B_{jk} B_{jm} m_{2,p}^{km}/S_2\right) t^2 + \cdots . \tag{4.28}$$

If the interaction between the spins is restricted to the 26 nearest neighbors then

$$\sum_{k, m(k \neq m)} B_{jk} B_{jm} m_{2,p}^{km}/S_2$$

is zero for $\vec{B}_0$ along the [001] and [111] directions. For $\vec{B}_0$ along the [110] direction the sum is (6–7)% of $m_{2,p}^{jj}$.[14] Accordingly, for short times we may for all three directions of $\vec{B}_0$ put

$$\langle B_p^{\rm loc} B_p^{\rm loc}(t)\rangle / \langle B_p^{\rm loc} B_p^{\rm loc}\rangle = f_p^{jj}(t) = e^{-m_{2,p}^{jj} t^2/2}. \tag{4.29}$$

τ_p is estimated from $f_p^{jj}(\tau_p) = e^{-1}$ giving

$$\tau_p = (2/m_{2,p}^{jj})^{1/2}. \tag{4.30}$$

$f_p(t)$ is obtained from the calculated $g_p(\omega)$ by Fourier inversion and is compared to the molecular-dynamics correlation functions in Figs. 1 and 3. The short-time behavior of $f_p(t)$ is seen to reproduce the experimental functions quite well as expected since a calculation of the first two time derivatives of Eq. (4.9) at $t = 0$ gives the correct values 0 and $-m_{2,p}^{jj}$, respectively. On the other hand, the long time behavior of $f_p(t)$ is less satisfactory. The transverse correlation functions have a long negative region and the longitudinal correlation functions decay to zero too fast, almost in an exponential fashion.

One shortcoming of the model is that the form of $f_p(t)$ is independent of the direction of $\vec{B}_0$—in contrast to the molecular-dynamics experiments and the ratio of moments $D_{2n,p}$ in Table II. This is seen by defining a new reduced time unit [compare Eq. (2.11)] as

$$X' = X\left(\sum_{k(\neq j)} (1 - 3\cos^2\theta_{jk})^2 / a_{jk}^6\right)^{-1/2}, \tag{4.31}$$

where $a_{jk} = r_{jk}/r_0$. In this unit we find $\tau_x = (\frac{54}{5})^{1/2}$, $\tau_z = 27^{1/2}$, $\Delta_x = (\frac{1}{27})^{1/2}$, and $\Delta_z = (\frac{4}{27})^{1/2}$. Accordingly, varying the direction of $\vec{B}_0$ simply changes the time scale for $f_p(t)$, but its form is conserved.

The agreement of $f_p(t)$ with the molecular-dynamics experiment varies therefore from one orientation of $\vec{B}_0$ to another. It is found that the overall agreement increases slightly in going from $\vec{B}_0$ along [001] via [110] to [111]. This becomes understandable by considering how the local field at the position of a given spin j is made up from the neighboring spins. For $\vec{B}_0$ along [001] the two neighboring spins i and k along [001] and [00$\bar{1}$] have an interaction, which is stronger by a factor of 2 than any other interaction involving j. On the other hand, for $\vec{B}_0$ along [111] the interaction between j and the neighboring spins are all of roughly the same magnitude, whereas the case with $\vec{B}_0$ along [110] largely lies in between. This means, that the basic assumption of the model, that the local field at spin j is independent of j at all times, is expected to be the least valid for $\vec{B}_0$ along [001], since in this case the time evolution of the orientations of the spins i and k depend to a relatively large extent upon the spin j, which in turn means that the local field at the spin j in this case is more dependent upon the history of j itself than in the case with $\vec{B}_0$ along [111].

V. BLUME-HUBBARD MODEL

Blume and Hubbard[8] (BH) have described a technique for calculation of the spin correlation functions of the Heisenberg model at high temperatures. BH found that the spin correlation functions predicted from their model are in excellent agreement with the molecular-dynamics calculations on Heisenberg spin system at high temperatures. Furthermore, in the last few years the technique of BH has also proved useful in the description of the dynamical behavior of other spin systems.[15–18] In this section we shall use their method to derive a set of equations for the spin correlation functions for a dipolar coupled spin system and we shall compare the result to the experiments described in Secs. II and III.

BH have shown that the correlation function $\langle AB(t)\rangle / \langle AB\rangle$ in the high-temperature limit may be calculated according to

$$\langle AB(t)\rangle / \langle AB\rangle = \langle \delta B(t)\rangle / \langle \delta B\rangle , \tag{5.1}$$

where

$$\langle \delta B(t)\rangle = -i \lim_{\epsilon \to 0+} \int_{-\infty}^{0} \langle [A(t'), B(t)]\rangle e^{\epsilon t'} dt'. \tag{5.2}$$

Introducing the spin operators

$$I_{\vec{q}}^{p}(t) = N^{-1} \sum_j I_{jp}(t) e^{i\vec{q}\cdot\vec{r}_j}, \quad p = x, y, z \tag{5.3}$$

we may express the wave-vector dependent correlation functions as

$$F_{\vec{q}}^{p}(t) = \frac{\langle I_{-\vec{q}}^{p} I_{\vec{q}}^{p}(t)\rangle}{\langle I_{-\vec{q}}^{p} I_{\vec{q}}^{p}\rangle} = \frac{\langle \delta I_{\vec{q}}^{p}(t)\rangle}{\langle \delta I_{\vec{q}}^{p}\rangle} . \tag{5.4}$$

The equation of motion for $\vec{I}_{\vec{q}}(t)$ is

$$\frac{d\vec{I}_{\vec{q}}(t)}{dt} = \gamma^2\hbar\sum_{\vec{q}_1} B_{\vec{q}_1}\vec{V}_{\vec{q}_1}\times\vec{I}_{\vec{q}-\vec{q}_1}, \tag{5.5}$$

where

$$\vec{V}_{\vec{q}_1} = (-\tfrac{1}{3}I^x_{\vec{q}_1}, -\tfrac{1}{3}I^y_{\vec{q}_1}, \tfrac{2}{3}I^z_{\vec{q}_1}) \tag{5.6}$$

and

$$B_{\vec{q}_1} = \sum_j B_{kj}\exp[i\vec{q}_1\cdot(\vec{r}_k - \vec{r}_j)]. \tag{5.7}$$

From Eq. (5.5) we derive a differential equation for $\delta\vec{I}_{\vec{q}}(t)$:

$$\delta\frac{d}{dt}\vec{I}_{\vec{q}}(t) = i\sum_{\vec{q}_1}\underline{h}_{\vec{q}\vec{q}_1}(t)\delta\vec{I}_{\vec{q}_1}(t), \tag{5.8}$$

where the tensor $\underline{h}_{\vec{q}\vec{q}_1}$ has the components

$$\begin{aligned}
&h^{pp}_{\vec{q}\vec{q}_1}(t) = 0, \quad p = x, y, z\\
&h^{xy}_{\vec{q}\vec{q}_1}(t) = i\gamma^2\hbar\tfrac{1}{3}(B_{\vec{q}_1} + 2B_{\vec{q}-\vec{q}_1})I^z_{\vec{q}-\vec{q}_1}(t) = -h^{yx}_{\vec{q}\vec{q}_1}(t),\\
&h^{xz}_{\vec{q}\vec{q}_1}(t) = i\gamma^2\hbar\tfrac{1}{3}(2B_{\vec{q}_1} + B_{\vec{q}-\vec{q}_1})I^y_{\vec{q}-\vec{q}_1}(t),\\
&h^{yz}_{\vec{q}\vec{q}_1}(t) = -i\gamma^2\hbar\tfrac{1}{3}(2B_{\vec{q}_1} + B_{\vec{q}-\vec{q}_1})I^x_{\vec{q}-\vec{q}_1}(t),\\
&h^{zx}_{\vec{q}\vec{q}_1}(t) = i\gamma^2\hbar\tfrac{1}{3}(B_{\vec{q}_1} - B_{\vec{q}-\vec{q}_1})I^y_{\vec{q}-\vec{q}_1}(t),\\
&h^{zy}_{\vec{q}\vec{q}_1}(t) = -i\gamma^2\hbar\tfrac{1}{3}(B_{\vec{q}_1} - B_{\vec{q}-\vec{q}_1})I^x_{\vec{q}-\vec{q}_1}(t).
\end{aligned} \tag{5.9}$$

In the derivation of Eq. (5.8) we have neglected all commutators of the type $[\delta I^p_{\vec{q}_1}, I^{p'}_{\vec{q}-\vec{q}_1}]$, where $p, p' = x, y, z$. However, it has been shown by Hubbard[15] that this approximation does not change the final result in the high-temperature limit, which we are discussing here.

From the formal solution of Eq. (5.8) we may express $F^p_{\vec{q}}(t)$ as

$$\begin{aligned}
F^p_{\vec{q}}(t) &= \langle\delta I^p_{\vec{q}}(t)\rangle / \langle\delta I^p_{\vec{q}}(0)\rangle\\
&= \left\langle\left[\exp_0\left(i\int_0^t \underline{h}(t')dt'\right)\delta\vec{I}(0)\right]^p_{\vec{q}}\right\rangle\Big/\langle\delta I^p_{\vec{q}}(0)\rangle,
\end{aligned} \tag{5.10}$$

where $\delta\vec{I}(0)$ is a $3N$-dimensional vector with components $\delta I^{p'}_{\vec{q}}(0)$, $p' = x, y, z$, $\vec{q} = \vec{q}_1, \vec{q}_2, \ldots, \vec{q}_N$, and the subscript 0 indicates a time ordering, and $[\cdots]^p_{\vec{q}}$ means the pth component with wave vector $\vec{q}$ of the vector $[\cdots]$. We now make use of the basic physical approximation in the theory of BH, namely the neglect of the detailed correlations of three or more spin operators, so that a cumulant expansion of Eq. (5.10) leads to

$$F^p_{\vec{q}}(t) = \left[\exp_0\left(-\int_0^t dt'\int_0^{t'} dt''\langle\underline{h}(t')\underline{h}(t'')\rangle\right)\right]^{pp}_{\vec{q}\vec{q}}, \tag{5.11}$$

where we have applied the initial condition

$$\langle\delta I^{p'}_{\vec{q}'}(0)\rangle = \langle\delta I^p_{\vec{q}}(0)\rangle\delta_{pp'}\delta_{\vec{q}\vec{q}'}. \tag{5.12}$$

In Eq. (5.11) $[\cdots]^{pp}_{\vec{q}\vec{q}}$ is the $p\vec{q}-p\vec{q}$ matrix element of the matrix $[\cdots]$. Differentiation of Eq. (5.11) yields

$$\dot{F}^p_{\vec{q}}(t) = -\left[\int_0^t dt'\langle\underline{h}(t)\underline{h}(t')\rangle\exp\left(-\int_0^t dt_1\int_0^{t_1} dt_2\langle\underline{h}(t_1)\underline{h}(t_2)\rangle\right)\right]^{pp}_{0\vec{q}\vec{q}}. \tag{5.13}$$

In order to account for the time ordering in Eq. (5.13) we make the approximation to the integral in the exponential function

$$\int_0^t dt_1\int_0^{t_1} dt_2 \simeq \int_0^{t'} dt_1\int_0^{t_1} dt_2 + \int_{t'}^t dt_1\int_{t'}^{t_1} dt_2, \tag{5.14}$$

i.e., we are neglecting the contribution from $\int_{t'}^t dt_1\int_0^{t'} dt_2$. We may now handle the time ordering in Eq. (5.13) explicitly as

$$\begin{aligned}
\dot{F}^p_{\vec{q}}(t) &= -\int_0^t dt'\left[\left\langle\underline{h}(t)\exp_0\left(-\int_{t'}^t dt_1\int_{t'}^{t_1} dt_2\langle\underline{h}(t_1)\underline{h}(t_2)\rangle\right)\underline{h}(t')\right\rangle\exp_0\left(-\int_0^{t'} dt_1\int_0^{t_1} dt_2\langle\underline{h}(t_1)\underline{h}(t_2)\rangle\right)\right]^{pp}_{\vec{q}\vec{q}}\\
&= -\sum_{p_1p_2p_3}\sum_{\vec{q}_1\vec{q}_2\vec{q}_3}\int_0^t dt'\left\langle h^{pp_1}_{\vec{q}\vec{q}_1}(t)\left[\exp_0\left(-\int_{t'}^t dt_1\int_{t'}^{t_1} dt_2\langle\underline{h}(t_1)\underline{h}(t_2)\rangle\right)\right]^{p_1p_2}_{\vec{q}_1\vec{q}_2} h^{p_2p_3}_{\vec{q}_2\vec{q}_3}(t')\right\rangle\\
&\quad\times\left[\exp_0\left(-\int_0^{t'} dt_1\int_0^{t_1} dt_2\langle\underline{h}(t_1)\underline{h}(t_2)\rangle\right)\right]^{p_3p}_{\vec{q}_3\vec{q}}
\end{aligned} \tag{5.15}$$

Since[8]

$$\left[\exp_0\left(-\int_0^{t'} dt_1\int_0^{t_1} dt_2\langle\underline{h}(t_1)\underline{h}(t_2)\rangle\right)\right]^{p_3p}_{\vec{q}_3\vec{q}} = \delta_{\vec{q}_3\vec{q}}\delta_{p_3p}F^p_{\vec{q}}(t'), \tag{5.16}$$

we may write Eq. (5.15) as

$$\dot{F}^{\rho}_{\vec{q}}(t) = -\sum_{\rho_1 \vec{q}_1} \int_0^t dt' \langle h^{\rho\rho_1}_{\vec{q}\vec{q}_1}(t) h^{\rho_1\rho}_{\vec{q}_1\vec{q}}(t') \rangle F^{\rho_1}_{\vec{q}_1}(t-t') F^{\rho}_{\vec{q}}(t'). \tag{5.17}$$

The various averages $\langle h^{\rho\rho_1}_{\vec{q}\vec{q}_1}(t) h^{\rho_1\rho}_{\vec{q}_1\vec{q}}(t') \rangle$ may be obtained from Eq. (5.9) so that we finally arrive at the following set of nonlinear integro differential equations which couple the longitudinal and transverse correlation functions as well as the various $\vec{q}$ vectors of the Brillouin zone.

$$\dot{F}^{x}_{\vec{q}}(t) = -\frac{\gamma^4\hbar^2}{27N} I(I+1) \sum_{\vec{q}_1} (B_{\vec{q}_1} + 2B_{\vec{q}-\vec{q}_1})^2 \int_0^t F^{z}_{\vec{q}-\vec{q}_1}(t-t') F^{x}_{\vec{q}_1}(t-t') F^{x}_{\vec{q}}(t') dt', \tag{5.18}$$

$$\dot{F}^{z}_{\vec{q}}(t) = -\frac{2\gamma^4\hbar^2}{27N} I(I+1) \sum_{\vec{q}_1} (B_{\vec{q}-\vec{q}_1} - B_{\vec{q}_1})(2B_{\vec{q}} + B_{\vec{q}-\vec{q}_1}) \int_0^t F^{x}_{\vec{q}-\vec{q}_1}(t-t') F^{x}_{\vec{q}_1}(t-t') F^{z}_{\vec{q}}(t')\, dt'. \tag{5.19}$$

From the solution of Eqs. (5.18) and (5.19) we may obtain the spin correlation functions in Eqs. (2.7) and (2.9) as

$$f^{jk}_{\rho}(t) = N^{-1} \sum_{\vec{q}} F^{\rho}_{\vec{q}}(t) \exp[i\vec{q} \cdot (\vec{r}_j - \vec{r}_k)]. \tag{5.20}$$

Before discussing the solution of Eqs. (5.18) and (5.19) we shall point out that the dependence of $\dot{F}^{\rho}_{\vec{q}}(t)$ upon $I(I+1)$ is linear so that a change in $I(I+1)$ changes the time scale of $F^{\rho}_{\vec{q}}(t)$ [and thereby $f^{jk}_{\rho}(t)$], but its form is retained. In terms of the coefficients, $m^{jk}_{2n,\rho}$, this means that $m^{jk}_{2n,\rho} \propto \hbar^{2n}[I(I+1)]^n$ and we may therefore expect that the theory reproduces experiments on classical spins better than those on finite spins.

In the classical limit we may express Eqs. (5.18) and (5.19) in reduced time units [Eq. (2.11)] as

$$\dot{F}^{x}_{\vec{q}}(t) = -(27N)^{-1} \sum_{\vec{q}_1} (B_{\vec{q}_1} + 2B_{\vec{q}-\vec{q}_1})^2 \int_0^t F^{z}_{\vec{q}-\vec{q}_1}(t-t') F^{x}_{\vec{q}_1}(t-t') F^{x}_{\vec{q}}(t') dt' \tag{5.21}$$

$$\dot{F}^{z}_{\vec{q}}(t) = -2(27N)^{-1} \sum_{\vec{q}_1} (B_{\vec{q}-\vec{q}_1} - B_{\vec{q}_1})(2B_{\vec{q}} + B_{\vec{q}-\vec{q}_1}) \int_0^t F^{x}_{\vec{q}-\vec{q}_1}(t-t') F^{x}_{\vec{q}_1}(t-t') F^{z}_{\vec{q}}(t') dt', \tag{5.22}$$

where $B_{\vec{q}}$ has been redefined as

$$B_{\vec{q}} = \sum_{j(\neq k)} (1 - 3\cos^2\theta_{jk}) \exp[i\vec{q} \cdot (\vec{r}_j - \vec{r}_k)] / a^3_{jk}. \tag{5.23}$$

Equations (5.21) and (5.22) have been solved numerically using the boundary conditions $F^{\rho}_{\vec{q}}(0) = 1$ and $\dot{F}^{\rho}_{\vec{q}}(0) = 0$. In this calculation the sum over $\vec{q}_1$ was approximated by a sum over 216 points in the Brillouin zone and the sum over j in Eq. (5.23) was restricted to the 26 nearest neighbors to k. The correlation functions obtained in this way are shown in Fig. 1–4 together with the molecular-dynamics results. It is also useful to compare the exact coefficients $m^{jk}_{2n,\rho}$ with those obtained from the model as

$$m^{jk}_{2n,\rho} = (-1)^n N^{-1} \sum_{\vec{q}} F^{\rho}_{\vec{q}}(2n, 0) \exp[i\vec{q} \cdot (\vec{r}_j - \vec{r}_k)], \tag{5.24}$$

where

$$F^{\rho}_{\vec{q}}(2n, 0) = \left. \frac{d^{2n} F^{\rho}_{\vec{q}}(t)}{dt^{2n}} \right|_{t=0}.$$

$F^{\rho}_{\vec{q}}(2n, 0)$ may be obtained from Eqs. (5.21) and (5.22), and are

$$F^{x}_{\vec{q}}(n, 0) = -(27N)^{-1} \sum_{\vec{q}_1} (2B_{\vec{q}-\vec{q}_1} + B_{\vec{q}_1})^2 \sum_{j=0}^{n-2} \sum_{k=0}^{n-2-j} \frac{(j+k)!}{j!\,k!} F^{z}_{\vec{q}-\vec{q}_1}(j, 0) F^{x}_{\vec{q}_1}(k, 0) F^{x}_{\vec{q}}(n-2-j-k, 0), \tag{5.25}$$

$$F^{z}_{\vec{q}}(n, 0) = -2(27N)^{-1} \sum_{\vec{q}_1} (B_{\vec{q}-\vec{q}_1} - B_{\vec{q}_1})(2B_{\vec{q}} + B_{\vec{q}-\vec{q}_1}) \sum_{j=0}^{n-2} \sum_{k=0}^{n-2-j} \frac{(j+k)!}{j!\,k!} F^{x}_{\vec{q}-\vec{q}_1}(j, 0) F^{x}_{\vec{q}_1}(k, 0) F^{z}_{\vec{q}}(n-2-j-k, 0). \tag{5.26}$$

Equations (5.25) and (5.26) show that all correlation functions have the correct value of $m^{jk}_{2,p}$, which is in agreement with the fact that none of the approximations made in deriving Eqs. (5.21) and (5.22) affects the coefficient to t^2.

For longer times the transverse correlation functions are not in good agreement with the molecular dynamics experiments as is evident from Fig. 1, where the transverse autocorrelation functions display large oscillations, which are absent in the experiments.[19] The position of the first extremum point of the transverse pair correlation functions in Fig. 2 is generally in good agreement with experiment, although the amplitude at this point is somewhat too large. For longer times the model predicts more extremum points than the experiments yield. The coefficients $m^{jk}_{4,x}$ and $m^{jk}_{6,x}$ are on the average smaller than the exact values by 17% and 37% for $j=k$, and by 24% and 46% for $j\neq k$, respectively.

In discussing the transverse correlation functions it is of special interest to consider $F^x_{\vec{q}=0}(t)$, which is the FID. This function has the zero points in fair agreement with experiments although the amplitude at the first minimum is roughly a factor 2.4 too large. The moments of the corresponding cw spectrum, M_4, M_6, and M_8 predicted from $F^x_{\vec{q}=0}$ $(2n,0)$ are smaller than the exact values by 20%, 42%, and 60%, respectively.

The longitudinal autocorrelation function in Fig. 3 represents the experiment well both in the short- and long-time region although the agreement with experiment for intermediate times is not so excellent as reported for the Heisenberg spin system at high temperatures. The good short-time agreement is also demonstrated in the values $m^{jj}_{4,z}$ and $m^{jj}_{6,z}$ which differ from the exact values by 4% and 8%.

The form of the longitudinal pair correlation functions in Fig. 4 seems to be well described by the model for times up to the first maximum point and $m^{jk}_{4,z}$ and $m^{jk}_{6,z}$ are found to differ from the exact values by 16% and 30%, respectively. For longer times the experimental functions do not permit a comparison due to the rather large numerical uncertainties.

Equation (5.22) may also be used to investigate $F^z_{\vec{q}}(t)$ in the hydrodynamical region, i.e., in the limit $\vec{q}\to 0, t\to\infty$. In this limit Eq. (5.22) becomes

$$\dot{F}^z_{\vec{q}}(t)=(27N)^{-1}\sum_{\vec{q}_1} B_{\vec{q}_1}\sum_k B_{jk} \times \sum_{p,p'=x,y,z}(\vec{r}_j-\vec{r}_k)_p(\vec{r}_j-\vec{r}_k)_{p'}\exp[-i\vec{q}_1\cdot(\vec{r}_j-\vec{r}_k)] \times\int_0^\infty [F^x_{\vec{q}_1}(t')]^2dt' F^z_{\vec{q}}(t)q_p q_{p'}, \tag{5.27}$$

from which we may identify the spin diffusion tensor as

$$D_{p,p'}=(27N)^{-1}\sum_{\vec{q}_1} B_{\vec{q}_1}\left(\frac{\partial^2}{\partial q_{1_p}\partial q_{1_{p'}}} B_{\vec{q}_1}\right) \times\int_0^\infty [F^x_{\vec{q}_1}(t')]^2dt'. \tag{5.28}$$

Numerical values of $D_{p,p'}$ may be found in Table IV. Generally, these values are 30% smaller than those derived from the density matrix theory of Lowe and Gade,[20] which is a satisfactory agreement considering the present state of art of experimental diffusion tensors.

VI. SUMMARY

The longitudinal and transverse auto- and pair correlation functions have been derived from a molecular-dynamics experiment for a system of classical spins interacting by a truncated dipolar coupling. The obtained correlation functions are used to examine the usefulness of two models to describe the dynamical behavior of the spin system.

First, we consider the Kubo and Toyabe model, which treats the local field at a given spin as a stochastic process independent of that spin, and we derive an infinite set of linear equations which permit the determination of the autocorrelation functions. The longitudinal correlation function is found to give the best agreement with experiment although it does not reproduce the observed long time dependence of the experimental correlation function.

Next, we adapt the general theory of Blume and Hubbard for the calculation of spin correlation functions to the spin system considered here. We make the same set of assumptions as Blume and Hubbard did and obtain a set of coupled nonlinear integro-differential equation for the transverse and longitudinal wave-vector-dependent correlation functions. Generally, we find this theory describes the longitudinal dynamics much better than the transverse dynamics. The transverse autocorrelation function has long-time oscillations whereas the experimental function is always positive and the FID has far too large oscillations to represent a better—or even as good—theoretical description of the FID than current theories. On the other hand the longitudinal correlation functions represent the dynamics rather well—although not as excellent as found for the Heisenberg spin system at high temperatures, and the spin diffusion tensor is within the accepted values.

APPENDIX

In this appendix we give analytical expressions for the coefficients $m^{jk}_{2n,p}$ in Eqs. (2.15) and (2.16). For convenience in writing we introduce $X=I(I+1)$ and the following lattice sums

$$S_n = N^{-1}\sum_{j,k} B^n_{jk}, \tag{A1}$$

and

$$R_{jk}(nm) = \sum_r B^n_{jr}B^m_{rk} \ (j\neq k); \tag{A2}$$

$$m^{jj}_{2,x} = \tfrac{5}{27}\gamma^4\hbar^2 S_2 X. \tag{A3}$$

$$m^{jj}_{4,x} = \frac{\gamma^8\hbar^4}{7290}\Big[X^2\Big(770S_2^2 - 164S_4 + 80\sum_k{}' B^2_{jk}R_{jk}(11)\Big) - 147XS_4\Big]. \tag{A4}$$

$$\begin{aligned} m^{jj}_{6,x} = \frac{\gamma^{12}\hbar^6}{729}\Big[\frac{X^3}{27}\Big(&2183S_2^3 - 152S_3^2 - 1464S_2S_4 + \frac{75708}{175}S_6 + 116S_2\sum_k{}' B^2_{jk}R_{jk}(11) + \frac{204}{5}\sum_k{}' B^4_{jk}R_{jk}(11) \\ &+ \frac{564}{5}\sum_k{}' B^3_{jk}R_{jk}(21) - \frac{2022}{5}\sum_k{}' B^2_{jk}R_{jk}(22) + 604\sum_k{}' B^2_{jk}R^2_{jk}(11) - 16\sum_k{}' B_{jk}R_{jk}(21)R_{jk}(11) \\ &- 56\sum_k{}' R^2_{jk}(21) - 16\sum_{k,p,q}{}' B_{jk}B_{jp}B_{jq}B_{kp}B_{kq}B_{pq}\Big) + \frac{X^2}{90}\Big(280S_3^2 - 4575S_2S_4 + \frac{64972}{35}S_6 \\ &+ 168\sum_k{}' B^4_{jk}R_{jk}(11) + 858\sum_k{}' B^3_{jk}R_{jk}(21) - 1134\sum_k{}' B^2_{jk}R_{jk}(22)\Big) + \frac{3728}{525}XS_6\Big]. \end{aligned} \tag{A5}$$

$$m^{jk}_{2,x} = \tfrac{4}{27}\gamma^4\hbar^2 B^2_{jk}X. \tag{A6}$$

$$m^{jk}_{4,x} = \frac{\gamma^8\hbar^4}{7290}\left[X^2(880S_2B^2_{jk} + 240R_{jk}(22) - 352B^4_{jk} + 380B^2_{jk}R_{jk}(11) + 80B_{jk}R_{jk}(21)) - 96XB^4_{jk}\right]. \tag{A7}$$

$$\begin{aligned} m^{jk}_{6,x} = \frac{\gamma^{12}\hbar^6}{729}\Big[\frac{X^3}{27}\Big(&\frac{31536}{35}B^6_{jk} - \frac{3884}{5}S_4B^2_{jk} + 2720S_2^2B^2_{jk} - \frac{11656}{5}S_2B^4_{jk} \\ &+ 280S_3B^3_{jk} - 744B^4_{jk}R_{jk}(11) - \frac{5576}{5}B^2_{jk}R_{jk}(31) + \frac{152}{5}B^3_{jk}R_{jk}(21) \\ &- \frac{808}{5}B_{jk}R_{jk}(41) - \frac{6768}{5}B^2_{jk}R_{jk}(22) - \frac{224}{5}B_{jk}R_{jk}(32) + 744B^2_{jk}R^2_{jk}(11) \\ &- 164B_{jk}R_{jk}(21)R_{jk}(11) + 1120S_2R_{jk}(22) - 656R_{jk}(42) + 300R_{jk}(22)R_{jk}(11) \\ &+ 8R_{jk}(33) - 240R^2_{jk}(21) + 2056S_2B^2_{jk}R_{jk}(11) + 128S_2B_{jk}R_{jk}(21) \\ &+ 840B_{jk}\sum_p{}' B^2_{jp}B_{kp}R_{jp}(11) + 540B_{jk}\sum_p{}' B^2_{jp}B_{kp}R_{kp}(11) - 112B_{jk}\sum_p{}' B_{jp}B_{kp}R_{jp}(21) \\ &- 280B^2_{jk}\sum_p{}' B^2_{kp}R_{jp}(11) + 380\sum_p{}' B^2_{jp}B^2_{kp}R_{jp}(11) + 60B_{jk}\sum_p{}' B_{kp}R_{jp}(22) \\ &+ 160\sum_p{}' B^2_{jp}R_{kp}(22) - 40B^2_{jk}\sum_p{}' B_{jp}B_{kp}R_{kp}(11) + 120\sum_p{}' B^2_{jp}B_{kp}R_{kp}(21) \\ &+ 8B^2_{jk}\sum_p{}' B^2_{jp}R_{jp}(11) - 200B_{jk}\sum_{p,q}{}' B_{jp}B_{jq}B_{kp}B_{kq}B_{pq} - 100\sum_{p,q}{}' B^2_{jp}B_{jq}B_{kp}B_{kq}B_{pq} \\ &+ 80\sum_{p,q}{}' B_{jp}B_{jq}B_{kp}B_{kq}B^2_{pq}\Big) + \frac{X^2}{90}(13304/7B^6_{jk} - 1348S_4B^2_{jk} - 2632S_2B^4_{jk} \\ &+ 600S_3B^3_{jk} - 575B^4_{jk}R_{jk}(11) - 1622B^2_{jk}R_{jk}(31) + 304B^3_{jk}R_{jk}(21) + 164B_{jk}R_{jk}(41) \\ &- 2106B^2_{jk}R_{jk}(22) + 622B_{jk}R_{jk}(32) - 760R_{jk}(42) - 70R_{jk}(33)) + \frac{356}{105}XB^6_{jk}\Big]. \end{aligned} \tag{A8}$$

$$m^{jj}_{2,z} = \tfrac{2}{27}\gamma^4\hbar^2 S_2 X. \tag{A9}$$

$$m^{jj}_{4,z} = \frac{\gamma^8\hbar^4}{7290}\left[X^2\left(260S_2^2 - 68S_4 - 160\sum_k{}' B_{jk}^2 R_{jk}(11)\right) - 84XS_4\right]. \tag{A10}$$

$$\begin{aligned} m^{jj}_{6,z} = \frac{\gamma^{12}\hbar^6}{729}\Bigg[\frac{X^3}{27}\Bigg(&788S_2^3 - 152S_3^2 - 564S_4S_2 + \frac{32328}{175}S_6 - 928S_2\sum_k{}' B_{jk}^2 R_{jk}(11) \\ &+ 336\sum_k{}' B_{jk}^4 R_{jk}(11) + 552\sum_k{}' B_{jk}^3 R_{jk}(21) - \frac{2166}{5}\sum_k{}' B_{jk}^2 R_{jk}(22) + 586\sum_k{}' B_{jk}^2 R_{jk}^2(11) \\ &- 304\sum_k{}' B_{jk} R_{jk}(21) R_{jk}(11) - 56\sum_k{}' R_{jk}^2(21) - 16\sum_{k,p,q}{}' B_{jk}B_{jp}B_{jq}B_{kp}B_{kq}B_{pq}\Bigg) \\ &+ \frac{X^2}{90}\Bigg(280S_3^2 - 2100S_4S_2 + \frac{30052}{35}S_6 + 1320\sum_k{}' B_{jk}^4 R_{jk}(11) + 300\sum_k{}' B_{jk}^3 R_{jk}(21) \\ &- 657\sum_k{}' B_{jk}^2 R_{jk}(22)\Bigg) + \frac{1748}{525}XS_6\Bigg]. \end{aligned} \tag{A11}$$

$$m^{jk}_{2,z} = -\tfrac{2}{27}\gamma^4\hbar^2 B_{jk}^2 X. \tag{A12}$$

$$m^{jk}_{4,z} = \frac{\gamma^8\hbar^4}{7290}\left[X^2(-320S_2B_{jk}^2 + 128B_{jk}^4 + 320B_{jk}^2 R_{jk}(11) - 160B_{jk}R_{jk}(21) + 60R_{jk}(22)) + 84XB_{jk}^4\right]. \tag{A13}$$

$$\begin{aligned} m^{jk}_{6,z} = \frac{\gamma^{12}\hbar^6}{729}\Bigg[\frac{X^3}{27}\Bigg(&-\frac{44928}{175}B_{jk}^6 + \frac{1228}{5}S_4B_{jk}^2 - 988S_2^2B_{jk}^2 + \frac{4832}{5}S_2B_{jk}^4 \\ &- 224S_3B_{jk}^3 - \frac{3144}{5}B_{jk}^4 R_{jk}(11) - 1216B_{jk}^2 R_{jk}(31) + \frac{2528}{5}B_{jk}^3 R_{jk}(21) \\ &+ \frac{704}{5}B_{jk}R_{jk}(41) + \frac{2016}{5}B_{jk}^2 R_{jk}(22) + \frac{1792}{5}B_{jk}R_{jk}(32) - 444B_{jk}^2 R_{jk}^2(11) \\ &+ 160B_{jk}R_{jk}(21)R_{jk}(11) + 220S_2R_{jk}(22) - 152R_{jk}(42) + 120R_{jk}(22)R_{jk}(11) \\ &+ 80R_{jk}(33) - 240R_{jk}^2(21) + 1912S_2B_{jk}^2R_{jk}(11) - 952S_2B_{jk}R_{jk}(21) \\ &- 132B_{jk}\sum_p{}' B_{jp}^2 B_{kp}R_{jp}(11) + 792B_{jk}\sum_p{}' B_{jp}^2B_{kp}R_{kp}(11) - 112B_{jk}\sum_p{}' B_{jp}B_{kp}R_{jp}(21) \\ &+ 224B_{jk}^2\sum_p{}' B_{kp}^2R_{jp}(11) - 160\sum_p{}' B_{jp}^2B_{kp}^2R_{jp}(11) - 48B_{jk}\sum_p{}' B_{kp}R_{jp}(22) - 20\sum_p{}' B_{jp}^2R_{kp}(22) \\ &- 616B_{jk}^2\sum_p{}' B_{jp}B_{kp}R_{kp}(11) + 120\sum_p{}' B_{jp}^2B_{kp}R_{kp}(21) + 8B_{jk}^2\sum_p{}' B_{jp}^2R_{jp}(11) \\ &+ 16B_{jk}\sum_{p,q}{}' B_{jp}B_{jq}B_{kp}B_{kq}B_{pq} + 80\sum_{p,q}{}' B_{jp}^2B_{jq}B_{kp}B_{kq}B_{pq} - 10\sum_{p,q}{}' B_{jp}B_{jq}B_{kp}B_{kq}B_{pq}^2\Bigg) \\ &+ \frac{X^2}{90}\Bigg(-\frac{30752}{35}B_{jk}^6 + 416S_4B_{jk}^2 + 1904S_2B_{jk}^4 - 480S_3B_{jk}^3 - 1448B_{jk}^4R_{jk}(11) - 2180B_{jk}^2R_{jk}(31) \\ &+ 916B_{jk}^3R_{jk}(21) + 128B_{jk}R_{jk}(41) + 657B_{jk}^2R_{jk}(22) + 964B_{jk}R_{jk}(32) \\ &- 220R_{jk}(42) + 200R_{jk}(33)\Bigg) - \frac{1748}{525}XB_{jk}^6\Bigg]. \end{aligned} \tag{A14}$$

In the above equations a prime on a summation sign indicates that none of the spin indices may take on the same value simultaneously.

It may be demonstrated that the coefficients in Eqs. (A3)–(A14) fulfill the following relations

$$m^{jj}_{2n,x} + \sum_{k(\neq j)} m^{jk}_{2n,x} = M_{2n} \tag{A15}$$

and

$$m^{jj}_{2n,z} + \sum_{k(\neq j)} m^{jk}_{2n,z} = 0, \quad n = 1,2,3 \tag{A16}$$

where M_{2n} is the $2n$th moment of the cw spectrum.

Numerical values of the coefficients $m^{jk}_{2n,p}$ ($p = x,z$) are given in Tables I and III. In these

tables each spin interacts with its 26 nearest neighbors only. However, it should be pointed out, that the numbers in Tables I and III do not exactly satisfy Eqs. (A15) and (A16), which is due to the fact that terms like $R_{jk}(22)$ may be nonzero, even if k is not among the 26 nearest neighbors to j.

[1] I. J. Lowe and R. E. Norberg, Phys. Rev. 107, 46 (1957).

[2] A. Abragam, *The Principles of Nuclear Magnetism* (Clarendon, Oxford, England, 1961), Chap. IV.

[3] M. Engelsberg and I. J. Lowe, Phys. Rev. B 10, 822 (1974).

[4] F. Lado, J. D. Memory, and G. W. Parker, Phys. Rev. B 4, 1406 (1971).

[5] O. Platz and R. G. Gordon, Phys. Rev. B 7, 4764 (1973).

[6] A. G. Redfield and W. N. Yu, Phys. Rev. 169, 443 (1968).

[7] R. Kubo and T. Toyabe, in *Magnetic Resonance and Relaxation*, edited by R. Blinc (North Holland, Amsterdam, 1967), p. 810.

[8] M. Blume and J. Hubbard, Phys. Rev. B 1, 3815 (1970).

[9] S. J. Knak Jensen and O. Platz, Phys. Rev. B 7, 31 (1973).

[10] S. J. Knak Jensen and E. Kjaersgaard Hansen, Phys. Rev. B 7, 2910 (1973).

[11] The long-time tail of the experimental $f_z^{jj}(t)$ is reproduced rather well if the principal values of the spin-diffusion tensor in Table IV are multiplied by 0.76.

[12] M. C. Wang and G. E. Uhlenbeck, Rev. Mod. Phys. 17, 323 (1945).

[13] P. W. Anderson, J. Phys. Soc. Jpn. 9, 316 (1954).

[14] This approximation is still good if the interaction between the spins is extended to 728 neighbors, since in this case the sum is 12% of $m_{2,p}^{jj}$ on the average.

[15] J. Hubbard, J. Phys. C 4, 53 (1971).

[16] F. B. McLean and M. Blume, Phys. Rev. B 7, 1149 (1973).

[17] C. Ebner and C. C. Sung, Phys. Rev. B 8, 5226 (1973).

[18] C. C. Sung, Phys. Rev. B 8, 5313 (1973).

[19] A preliminary report on the transverse autocorrelation functions was given by S. J. Knak Jensen and E. Kjaersgaard Hansen, in *Proceedings of the First Specialized Colloque Ampere*, edited by J. W. Hennel (Institute of Nuclear Physics, Cracow, Poland, 1973), p. 200.

[20] I. J. Lowe and S. Gade, Phys. Rev. 156, 817 (1967).